Organic Electrodes Based on Grafted Oligothiophene Units in Ultrathin, Large-Area Molecular Junctions

ARTICLE *in* JOURNAL OF THE AMERICAN CHEMICAL SOCIETY · DECEMBER 2011

Impact Factor: 12.11 · DOI: 10.1021/ja209914d · Source: PubMed

5 AUTHORS, INCLUDING:

Pascal Martin
Paris Diderot University
47 PUBLICATIONS **415** CITATIONS
SEE PROFILE

Maria Luisa Della Rocca
Paris Diderot University
27 PUBLICATIONS **312** CITATIONS
SEE PROFILE

Philippe Lafarge
Paris Diderot University
29 PUBLICATIONS **1,116** CITATIONS
SEE PROFILE

Jean Christophe Lacroix
Paris Diderot University
133 PUBLICATIONS **2,726** CITATIONS
SEE PROFILE

JACS
JOURNAL OF THE AMERICAN CHEMICAL SOCIETY

Communication

pubs.acs.org/JACS

Organic Electrodes Based on Grafted Oligothiophene Units in Ultrathin, Large-Area Molecular Junctions

Pascal Martin,[†] Maria Luisa Della Rocca,[‡] Anne Anthore,[‡,§] Philippe Lafarge,[‡] and Jean-Christophe Lacroix*,[†]

[†]Université Paris Diderot, Sorbonne Paris Cité, ITODYS, UMR 7086 CNRS, 15 rue J-A de Baïf, 75205 Paris Cedex 13, France
[‡]Université Paris Diderot, Sorbonne Paris Cité, MPQ, UMR 7162 CNRS, 75205 Paris Cedex 13, France

ABSTRACT: Molecular junctions were fabricated with the combined use of electrochemistry and conventional CMOS tools. They consist of a 5−10 nm thick layer of oligo(1-(2-bisthienyl)benzene) between two gold electrodes. The layer was grafted onto the bottom electrode using diazonium electroreduction, which yields a stable and robust gold−oligomer interface. The top contact was obtained by direct electron-beam evaporation on the molecular layers through masks defined by electron-beam lithography. Transport mechanisms across such easily p-dopable layers were investigated by analysis of current density−voltage (J−V) curves. Application of a tunneling model led to a transport parameter (thickness of ∼2.4 nm) that was not consistent with the molecular thickness measured using AFM (∼7 nm). Furthermore, for these layers with thicknesses of 5−10 nm, asymmetric J−V curves were observed, with current flowing more easily when the grafted electrode was positively polarized. In addition, J−V experiments at two temperatures (4 and 300 K) showed that thermal activation occurs for such polarization but is not observed when the bias is reversed. These results indicate that simple tunneling cannot describe the charge transport in these junctions. Finally, analysis of the experimental results in term of "organic electrode" and redox chemistry in the material is discussed.

The development of molecular electronic junctions is driven by the prospect of higher density and new functionalities in microelectronics.[1] To maintain the cost-effective, massively parallel process of the complementary metal oxide semiconductor (CMOS) industry, the hybrid approach of incorporating organic layers between metallic electrodes seems to be promising. For the development of such hybrid systems, the molecular components must be compatible with CMOS fabrication processes. The layers should thus be stable at operating temperatures and during the fabrication steps through various vapor deposition process and/or electronic or optical lithography. To date, the majority of molecular junctions have been based on gold−thiol self-assembled and Langmuir−Blodgett films.[2,3] These films are unfortunately fragile. In many cases, the deposition of the top electrode is the key point of the fabrication, and the diffusion of metallic atoms through the organic layer to create a short circuit is a severe drawback. Even though specific strategies such as liquid top coat contact[4,5] have been used, it remains very difficult to deposit a second top coat electrode on such fragile layers. A clear breakthrough was reported by McCreery et al.[6] with the incorporation of organic layers in molecular junctions using the reduction of diazonium salts. Such an electrochemical process yields ultrathin organic layers grafted covalently onto the substrate.[7,8] These layers are much more robust than those obtained using SAMs on gold, and copper/gold top electrodes can be deposited. The devices exhibit enhanced stability and reproducibility. Changing the thickness of the layer in the 1−5 nm range and the type of π-conjugated system thus became possible, and many important results have thus been reported.[9−11] Most devices exhibit symmetric current density−voltage (J−V) curves, with J and the junction conductance decreasing exponentially with the film thickness. This clearly shows that tunneling transport occurs through such films, although for increasing thickness the agreement between simple tunneling models and the experimental results is more difficult.[12] Overall, transport measurements on such devices at various temperatures show that reorganization, redox chemistry, and ion motions are not involved in electron transport.

When the film thickness is 5−10 nm, the charge transport mechanism is likely to change. Indeed, a tunneling-to-hopping transition has been experimentally observed using an STM configuration above 5 nm.[13,14] Hopping may thus also be observed in large-area molecular junction of such thicknesses but requires doping in the materials for some bias.

In this work, we studied molecular junctions incorporating 5−10 nm thick organic layers based on oligothiophenes grafted onto gold electrodes using diazonium electroreduction. Such layers exhibit reversible on/off electrochemical switching controlled by the redox state of the oligomer[15,16] and may thus be of interest for solid-state molecular electronic junctions. First, we applied an all-CMOS technology for junction fabrication to check the molecular robustness. Second, we investigated their J−V characteristics to explore whether quantum tunneling still remains the dominant charge transport mechanism or if the use of these easily dopable layers can yield new device functionality not seen with thinner films.

Throughout the process, we used conventional solid-state fabrication techniques that are fully compatible with semiconductor industrial processing. The crossbar molecular junction fabrication process is summarized in Figure 1A. The bottom electrode consisted of a Ti (2 nm)/Au (50 nm) layer designed by e-beam lithography using a PMMA resist mask (Figure 1A, steps i and ii). Oligo(BTB) [BTB = 1-(2-bisthienyl)benzene] was electrochemically grafted on this electrode (step iii).

Received: October 21, 2011
Published: December 8, 2011

dx.doi.org/10.1021/ja209914d | J. Am. Chem.Soc. 2012, 134, 154−157

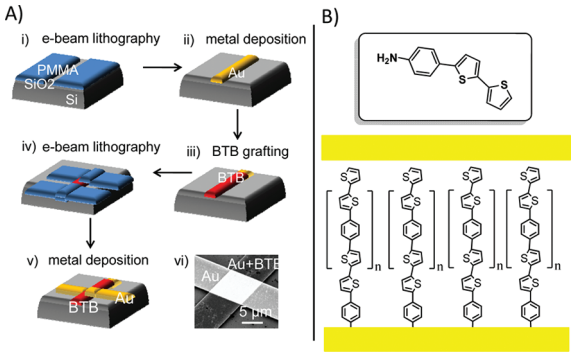

Figure 1. (A) Schematic diagram of the different steps of the fabrication process of metal/molecule/metal junctions. (B) Structure of the BTAB precursor and a schematic representation of oligo(BTB) layer between the two electrodes.

A second PMMA resist mask was then fabricated on the molecular layer by e-beam lithography (step iv), and the top contact was deposited by direct electron-beam evaporation of Ti (2 nm)/Au (50 nm) through this mask onto the molecular layer (step v). Particular attention was paid to the experimental conditions during Ti evaporation to avoid the formation of TiO_2 ($P < 3 \times 10^{-7}$ Torr, evaporation rate = 0.1 nm/s, and long pre-evaporation before deposition to pump out residual O_2).[17,18] In situ formation of TiO_2 through a chemical reaction with residual water or oxygenated species trapped in the organic film remained possible, but the TiO_2 layer thickness could not exceed 2 nm. Each sample consisted of eight junctions with areas varying from 5 μm × 5 μm to 100 μm × 100 μm.

Figure 2A shows the electroreduction of the diazonium salt generated in situ from the 1-(2-bisthienyl)-4-aminobenzene (BTAB)

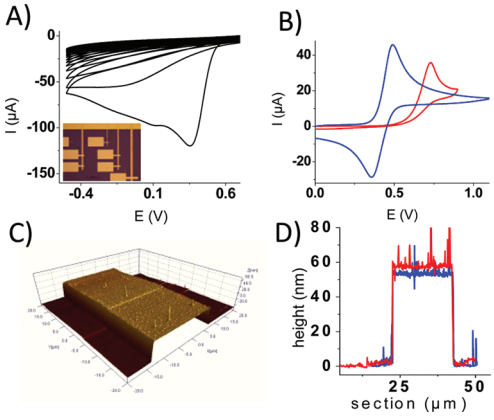

Figure 2. (A) CV of BTAB electroreduction in CH_3CN.[19] Inset: image of seven molecular junctions. (B) Fc electrochemical responses (10^{-3} M solution in CH_3CN) on bare (blue curve) and oligo(BTB)-modified (red curve) electrodes. (C) 3D AFM image of a BTB-modified 20 μm "finger". (D) Cross sections of bare (blue curve) and modified (red curve) 20 μm "fingers".

precursor. Cyclic voltammetry (CV) showed an irreversible wave during the first scan, corresponding to the formation of aryl radicals. In the following scans, the current dropped as the electrode surface was passivated by the grafting of an ultrathin film described as a BTB multilayer or, more correctly, as an oligo(BTB) layer.[19] The films were electroactive and could be easily p-doped at a potential close to 0.5 V vs SCE. As a consequence, the film conductance could be switched, and diodelike behavior with a strong rectification ratio was observed in the electrochemical response of several outer-sphere redox probes on oligo(BTB) electrodes. As an example, Figure 2B compares the electroactivity of ferrocene (Fc) on bare and oligo(BTB)-modified electrodes. In the potential window where Fc redox reactions were seen on a bare electrode, no current was observed on the oligo(BTB) electrode. The organic layer was insulating and totally blocked electron transfer toward Fc. Tunneling across such an insulating layer was thus inefficient, as the average tunneling distance across the film was too large. However, above 0.5 V vs SCE, the film conductance was switched to a conductive state, and the Fc oxidation current dramatically increased. During the backward scan, the film was switched back to an insulating state and no Fc^+ reduction peak was observed.

Atomic force microscopy (AFM) measurements were done to estimate the film thickness on the electrodes used as the bottom contact in the junctions. Figure 2C shows the topography of the BTB-modified surface before step iv, with an average roughness of ~1.5 nm. The thickness was 7 ± 2 nm, as measured by comparison of the cross sections before and after the grafting (Figure 2D).

Transport properties were measured at room temperature with the bottom contact grounded and the voltage applied to the top contact. We observed reproducible $J-V$ curves when the voltage sweep rate was varied from 0.08 to 8 V/s. The yield, defined as the percentage of devices that showed neither short contacts nor resistive behavior, was 33%. Though this value could be improved, it shows the compatibility between a full CMOS technology and the BTB molecular layer, revealing its intrinsic robustness. Figure 3A shows a representative $J-V$

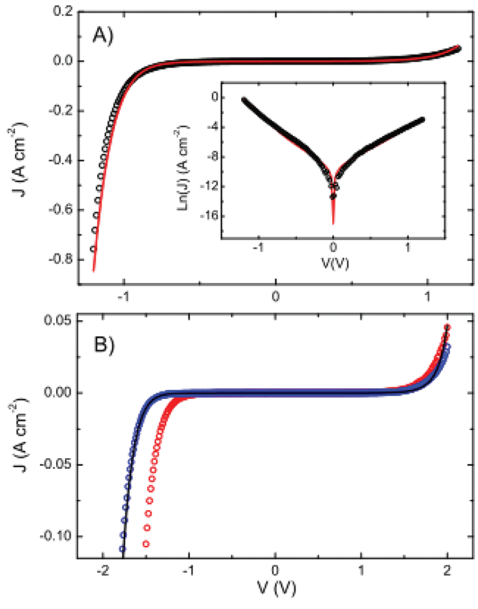

Figure 3. (A) $J-V$ experimental data (black ○) for a 100 μm × 100 μm molecular junction with a BTB thickness of 7 ± 2 nm compared with the theoretical fit described in the text (red line). Negative voltage corresponds to the Au/BTB being positive relative to the top electrode. Inset: logarithmic plot of the same $J-V$ curve. (B) $J-V$ experimental data for a 20 μm × 20 μm junction at 300 K (red ○) and 4 K (blue ○). The black solid line shows the best fit, which was obtained using d = 2.61 nm, ϕ_L = 1.16 eV, and ϕ_R = 2.14 eV.

curve measured with the device structure shown in Figure 1. The highly nonlinear shape of the $J-V$ curve with a linear

dx.doi.org/10.1021/ja209914d | J. Am. Chem.Soc. 2012, 134, 154–157

dependence at low voltage and an exponential increase at large voltage (see the Figure 3A inset) is a characteristic feature of quantum-mechanical tunneling in molecular junctions,[1] indicating the absence of metal shorts in the junctions. On the contrary, the strong asymmetry observed is rarely seen in the literature for such ultrathin films, although it has been reported in earlier studies[20,21] since the seminal publications of Aviram and Ratner[22] on molecular rectifiers.

The Simmons model[23] is the most common approach for describing tunneling in molecular devices. In the present case, this model is not suitable because it cannot account for asymmetric $J-V$ curves. A model based on tunneling through an asymmetric trapezoidal potential barrier was used to describe transport in our junctions. To fit the experimental data, we used the following expression for the current density J as a function of voltage V:

$$J = \frac{4\pi me}{h^3} \int_0^{+\infty} \mathrm{d}E\, [f_1(E) - f_2(E)] \int_0^E T(E_x)\, \mathrm{d}E_x$$

where e is the elementary charge, m is the electron mass, h is Planck's constant, $f_1(E)$ and $f_2(E)$ are the Fermi–Dirac distributions corresponding to the electrodes, and $T(E_x)$ is the WKB transmission probability, given by

$$T(E_x) = \exp\left\{ -\frac{4\pi}{h} \int_{s_1}^{s_2} [2m(\phi(x, V) - E_x)]^{1/2}\, \mathrm{d}x \right\}$$

where s_1 and s_2 are the classical turning points at the energy E_x and $\phi(x, V)$ is the potential barrier shape, given by $\phi(x, V) = \phi_L + (x/d)(\phi_R - eV - \phi_L)$, where d is the barrier thickness and ϕ_L and ϕ_R are the barrier heights on each side at zero applied voltage. We performed an exact numerical calculation of the transmission probability, in contrast to the approximations used in the Simmons model. The red line in Figure 3A shows the least-squares fit to the exact asymmetric potential barrier model using d, ϕ_L and ϕ_R as free parameters. The best fitting parameters (minimized χ^2) were found to be d = 2.42 nm, ϕ_L = 0.70 eV, and ϕ_R = 1.95 eV.

Despite the relatively low values of the current density, it is clear that the effective tunneling barrier width (2.42 nm) is smaller than the molecular layer thickness measured prior to the deposition of the top contact electrode (7 ± 2 nm). In fact, tunneling through a barrier thicker than 5 nm would result in hardly measurable currents. Two features can explain this discrepancy: (i) penetration of the top electrode into the organic layer during the top contact deposition process and (ii) doping of the organic layer at increasing bias to extend the conducting "contact" into the molecular layer. The first interpretation is not consistent with the strong asymmetric behavior observed, since thinner films based on SAMs or diazonium deposition in similar configurations usually exhibit symmetric $J-V$ curves.[13,24−27] It is also not consistent with the value of the junction resistance at low voltage in the linear part of the $J-V$ curve. Indeed, many groups have demonstrated that the junction resistance (R) is an exponential function of molecular thickness that is consistent with an expression derived for nonresonant tunneling transport: $R = R_0 \exp(\beta d)$, where R_0 is the contact resistance, β is the attenuation factor (2.5−3 nm^{-1} for π-conjugated molecules[12]), and d is the molecular thickness. In the case of Figure 3A, R is $2.5 \times 10^5\ \Omega\ \mathrm{cm}^2$, which yields an estimated effective tunneling barrier width of >7 nm at low bias, in line with the real thickness of the layer. This contradiction suggests that the effective tunneling barrier width is bias-dependent and that doping of the organic layer occurs. Indeed, polarons in such an organic oligomer are highly delocalized, with lengths close to 5 nm.[28] Doping of the organic layer may thus yield an organic conductor, extending the metallic interface from the grafted side in the oligoBTB layer and resulting in an effective tunneling barrier width smaller than the film thickness.

Within the frame of the model used, the asymmetric shape of the $J-V$ curve can be attributed to a lower effective barrier height ϕ_L (relative to ϕ_R) on the Au/BTB-grafted side of the molecular junction. It is tempting to attribute this result to the differences in the two contact interfaces. The injection barriers are indeed in good agreement with such idea, since a covalent Au–BTB bond should cause a lower injection barrier and thus a higher current for the negative bias. However, many reports on devices with thicknesses of 1–5 nm, have shown that with two different interfaces, the general shape of the $J-V$ curve remains symmetric even when two metals of very different work function are used as electrodes.[24−27] A more plausible interpretation is a change in the charge transport processes with a change in the bias polarity, from tunneling at one bias to hopping combined with tunneling at the opposite bias. Indeed, such an asymmetric response is comparable to the "anomalous" effect reported by McCreery in the case of an insulating layer between PPF and TiO_2.[18,29] It is also close to that reported by Whitesides and co-workers in junctions incorporating SAMs of alkanethiolates having Fc termini, whereas similar junctions without Fc do not rectify.[5] The common constituent of these rectifying devices is that they incorporate easily dopable moieties (TiO_2 and Fc, respectively) in an asymmetric configuration. In the present case, the BTB moieties are easily p-dopable species that are disposed in the device in an asymmetric configuration.

To obtain a deeper understanding of the nature of the transport mechanism through this organic layer, we performed the $J-V$ measurement at two different temperatures. Electron transport via tunneling is known to be a temperature-independent process, while many conduction mechanisms, such as hopping, have a marked dependence of the current density on temperature. Figure 3B shows $J-V$ curves for the BTB junction taken at two temperatures, 4 and 300 K. Two different regions were observed. At positive bias, the current density was slightly dependent on temperature, while a strong shift of current density was observed below −1 V. This indicates that a nonadiabatic process began to operate at negative bias. Recent results obtained for junctions containing thicker layers (4.7 nm) of azobenzene and nitroazobenzene have shown a temperature dependence in the range 200–330 K with an activation barrier of 35–102 meV.[12,25,30] According to the authors, this is consistent with effects derived from the Fermi distribution of the electrons in the contacts and not with molecular reorganization or redox reactions. Such an explanation is not compatible with an activation process observed only for negative bias. We believe that in the present case a change in the transport mechanism occurs, including a two-step mechanism as recently proposed by Luo et al.[9] for a redox-active molecular wire in combination with a bias polarity dependence as observed in SAM-containing ferrocene units.[5] If we assume that the characteristics of the molecular devices are indeed dominated by the chemical composition of the layers, our results suggest that a part of the organic layer can participate in hopping/doping transport when another part participates in tunneling transport.

To interpret our experimental results, a possible charge transport mechanism is proposed in Figure 4. At low bias, the layer is undoped and the tunneling barrier is 7 nm, resulting in a

dx.doi.org/10.1021/ja209914d | J. Am. Chem.Soc. 2012, 134, 154–157

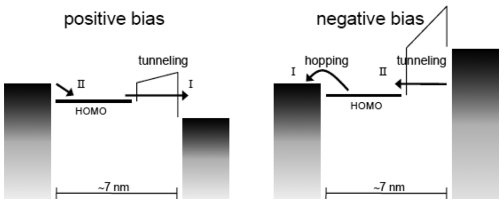

Figure 4. Energy level diagram and mechanism of charge transport across the BTB junction. Arrows show the electron transport direction.

large junction resistance. For both positive and negative bias, some BTB moieties are oxidized, generating BTB^+ moieties. In view of the polaron length of 4−5 nm,[28] the remaining part of the molecule acts as a tunneling barrier with an effective thickness of 2−3 nm, consistent with the extracted fitting values. At positive bias, the Fermi level of the top electrode decreases to below the value of the HOMO level. Thus, we speculate that a two-step process occurs: the first step (step I in Figure 4) involves tunneling of an electron from the HOMO level of the BTB layer to the top electrode, resulting in a p-doped layer (BTB^+), and the second step (step II in Figure 4) involves transfer of an electron from the energetically accessible states of the bottom electrode to the BTB^+. Electrons can occupy this level without any activation. For negative bias, a different two-step process governs the electron transport: the first is hopping from the molecular HOMO levels to the electronically accessible states of the base electrode, and the second is tunneling through the potential barrier. Clearly this first step has an activation energy that is temperature-dependent. Following this scheme, hopping is effective only at negative bias. For both polarities, tunneling is still the rate-limiting step in the transport mechanism and controls the whole process. The lifetime of BTB^+ moieties is probably short, and their amount remains unknown. The thin TiO_2 layer that may be generated in situ could help in the doping process. Finally, caution must be exercised, as this plausible mechanism may not the only possible interpretation of the observed asymmetric conduction. Further experiments on films of various thicknesses should be performed to validate our model.

In summary, we have reported a new molecular junction based on an easily p-dopable oligothiophene layer which is stable during the CMOS steps of the fabrication. The organic layer thickness was 7 nm, which is above the 5 nm layer thickness where the transition from simple tunneling to hopping has been demonstrated in the STM configuration. $J-V$ curves showed a rectifying behavior with a small rectification ratio. Transport measurements as a function of temperature suggested a different charge transport mechanism across the Au−BTB−Au junctions depending on the bias polarity, with tunneling supplemented by hopping at low temperature and negative bias. The observed behavior is potentially useful for constructing original organic electrodes.

AUTHOR INFORMATION

Corresponding Author

lacroix@univ-paris-diderot.fr

Present Address

[§]LPN-CNRS, route de Nozay, 91460 Marcoussis, France.

ACKNOWLEDGMENTS

This work was supported by the French Agence Nationale de la Recherche under Grant ANR-08-BLAN-0186-03. Prof. R. McCreery is warmly thanked for fruitful discussions.

REFERENCES

(1) McCreery, R. L. *Chem. Mater.* **2004**, *16*, 4477.
(2) Chabinyc, M. L.; Chen, X.; Holmlin, R. E.; Jacobs, H.; Skulason, H.; Frisbie, C. D.; Mujica, V.; Ratner, M. A.; Rampi, M. A.; Whitesides, G. M. *J. Am. Chem. Soc.* **2002**, *124*, 11730.
(3) Stewart, D. R.; Ohlberg, D. A. A.; Beck, P. A.; Chen, Y.; Williams, R. S.; Jeppesen, J. O.; Nielsen, K. A.; Stoddart, J. F. *Nano Lett.* **2003**, *4*, 133.
(4) Weiss, E. A.; Chiechi, R. C.; Kaufman, G. K.; Kriebel, J. K.; Li, Z.; Duati, M.; Rampi, M. A.; Whitesides, G. M. *J. Am. Chem. Soc.* **2007**, *129*, 4336.
(5) Nijhuis, C. A.; Reus, W. F.; Barber, J. R.; Dickey, M. D.; Whitesides, G. M. *Nano Lett.* **2010**, *10*, 3611.
(6) Ru, J.; Szeto, B.; Bonifas, A.; McCreery, R. L. *ACS Appl. Mater. Interfaces* **2010**, *2*, 3693.
(7) Mahouche-Chergui, S.; Gam-Derouich, S.; Mangeney, C.; Chehimi, M. M. *Chem. Soc. Rev.* **2011**, *40*, 4143.
(8) Belanger, D.; Pinson, J. *Chem. Soc. Rev.* **2011**, *40*, 3995.
(9) Luo, L.; Benameur, A.; Brignou, P.; Choi, S. H.; Rigaut, S.; Frisbie, C. D. *J. Phys. Chem. C* **2011**, *115*, 19955.
(10) Chen, X.; Jeon, Y.-M.; Jang, J.-W.; Qin, L.; Huo, F.; Wei, W.; Mirkin, C. A. *J. Am. Chem. Soc.* **2008**, *130*, 8166.
(11) Engelkes, V. B.; Beebe, J. M.; Frisbie, C. D. *J. Am. Chem. Soc.* **2004**, *126*, 14287.
(12) Bergren, A. J.; McCreery, R. L.; Stoyanov, S. R.; Gusarov, S.; Kovalenko, A. *J. Phys. Chem. C* **2010**, *114*, 15806.
(13) Choi, S. H.; Risko, C.; Delgado, M. C. R.; Kim, B.; Brédas, J.-L.; Frisbie, C. D. *J. Am. Chem. Soc.* **2010**, *132*, 4358.
(14) Hines, T.; Diez-Perez, I.; Hihath, J.; Liu, H.; Wang, Z.-S.; Zhao, J.; Zhou, G.; Müllen, K.; Tao, N. *J. Am. Chem. Soc.* **2010**, *132*, 11658.
(15) Fave, C.; Leroux, Y.; Trippé, G.; Randriamahazaka, H.; Noel, V.; Lacroix, J.-C. *J. Am. Chem. Soc.* **2007**, *129*, 1890.
(16) Stockhausen, V.; Ghilane, J.; Martin, P.; Trippé-Allard, G.; Randriamahazaka, H.; Lacroix, J.-C. *J. Am. Chem. Soc.* **2009**, *131*, 14920.
(17) McCreery, R.; Dieringer, J.; Solak, A. O.; Snyder, B.; Nowak, A. M.; McGovern, W. R.; DuVall, S. *J. Am. Chem. Soc.* **2003**, *125*, 10748.
(18) McCreery, R.; Dieringer, J.; Solak, A. O.; Snyder, B.; Nowak, A. M.; McGovern, W. R.; DuVall, S. *J. Am. Chem. Soc.* **2004**, *126*, 6200.
(19) Fave, C.; Noel, V.; Ghilane, J.; Trippé-Allard, G.; Randriamahazaka, H.; Lacroix, J. C. *J. Phys. Chem. C* **2008**, *112*, 18638.
(20) Metzger, R. M.; Panetta, C. A. *New J. Chem.* **1991**, *15*, 209.
(21) Martin, A. S.; Sambles, J. R.; Ashwell, G. J. *Phys. Rev. Lett.* **1993**, *70*, 218.
(22) Aviram, A.; Ratner, M. A. *Chem. Phys. Lett.* **1974**, *29*, 277.
(23) Simmons, J. G. *J. Appl. Phys.* **1963**, *34*, 1793.
(24) Akkerman, H. B.; Blom, P. W. M.; de Leeuw, D. M.; de Boer, B. *Nature* **2006**, *441*, 69.
(25) Bonifas, A. P.; McCreery, R. L. *Nat. Nanotechnol.* **2010**, *5*, 612.
(26) Nijhuis, C. A.; Reus, W. F.; Whitesides, G. M. *J. Am. Chem. Soc.* **2009**, *131*, 17814.
(27) Preiner, M. J.; Melosh, N. A. *Appl. Phys. Lett.* **2008**, *92*, No. 213301.
(28) Lacroix, J. C.; Chane-Ching, K. I.; Maquère, F.; Maurel, F. *J. Am. Chem. Soc.* **2006**, *128*, 7264.
(29) Yan, H.; McCreery, R. L. *ACS Appl. Mater. Interfaces* **2009**, *1*, 443.
(30) Anariba, F.; McCreery, R. L. *J. Phys. Chem. B* **2002**, *106*, 10355.